The Evolution and Transmission Dynamics of H3N2 Influenza Virus Identified in A Respiratory Disease Outbreak in Companion Dogs in Alabama, USA

Shakiba Kazemian
Auburn University
Sana Tamim
National Institute of Health
Peter Neasham
Auburn University
Samiah Kanwar
Aga Khan University
Kevin Zhong
Auburn University
Kelly Chenoweth
Auburn University
Andrea Perkins
Auburn University
Miria Criado
Auburn University
Paul Walz
Auburn University
Chengming Wang
Auburn University
Nidia Trovao
Fogarty International Center
Constantinos Kyriakis
csk0021@auburn.edu
Auburn University

Article

Keywords: phylodynamic, canine influenza, reassortment, surveillance

Posted Date: April 20th, 2026

DOI: https://doi.org/10.21203/rs.3.rs-9053609/v1

Additional Declarations: No competing interests reported.

Abstract

Canine Influenza Virus H3N2, initially of avian origin, emerged in Asia around 2005–2007 and subsequently spread globally, reaching the United States in 2015. Despite initial containment efforts, H3N2 CIV re-emerged in several US states in 2023. This study investigates the evolution and transmission dynamics of H3N2 CIV identified in companion dogs during an outbreak in Alabama, USA, between August and October 2022. We performed whole-genome sequencing on five H3N2 CIV isolates and conducted phylodynamic modeling, incorporating 100 global H3N2 CIV genomes per segment. Phylogenetic reconstruction showed the Alabama strains formed distinct, tightly clustered groups, suggesting recent common ancestry and localized evolution. Phylogeographic inference revealed discordant origins for different gene segments. The HA, MP, NP, NS, and PA genes traced ancestry to California strains, the NA gene to Florida strains, and the PB1 and PB2 genes to Illinois strains. This genomic incongruence strongly indicates that the Alabama outbreak strain emerged through a reassortment event involving viruses from these three geographically distinct regions. The findings highlight reassortment as a crucial mechanism driving CIV H3N2 evolution and spread, likely facilitated by the movement of infected dogs. Low canine vaccination requires continued surveillance and shelter-focused vaccination to control CIV outbreaks and monitor adaptation.

INTRODUCTION

Influenza A viruses (IAVs) are a class of segmented, negative-sense RNA viruses that are members of the *Orthomyxoviridae* family. The genome of IAVs consists of 8 segments and can encode up to 18 viral proteins [1]. These proteins are encoded by the following viral gene segments: hemagglutinin (HA), nucleoprotein (NP), neuraminidase (NA), matrix proteins (MP), nonstructural proteins (NS), two basic polymerases (PB1 and PB2), and one acidic polymerase (PA) [2]. IAVs evolve rapidly, producing antigenic and genetic diversity *via* antigenic drift [3]. Notably, due to the high error rates and poor proofreading capabilities of the viral RNA-dependent RNA polymerase, antigenic drift leads to the generation of antigenic variants through different mutations. This process, driven by the high error rate and limited proofreading ability of the viral RNA-dependent RNA polymerase, produces antigenic variants *via* accumulated mutations. In addition, reassortment of genomic segments between co-infecting strains facilitates antigenic shift, leading to the emergence of novel strains [4]. Cross-species transmission events may occur and result in either isolated infections or larger outbreaks, often originating from avian reservoirs before adapting to mammalian hosts [5].

IAVs have long been known to circulate in humans and other mammals, but dogs were resistant to IAVs, even in the face of evidence of exposure and/or spillover infections [6]. Canine Influenza Viruses (CIVs) belong to the same genus as IAVs and include subtypes of

H3N8 and H3N2 that currently circulate in dog populations [7] and have been undergoing several host adaptations [8]. The canine pandemic-causing H3N8 CIV virus was initially discovered in Florida in 2004, and before that, there were no records of CIV infections [5, 9]. When H3N2 CIV was first discovered in South Korea in 2007, it was identified as avian origin [10]. According to a later study, avian-origin H3N2 CIV was already circulating in China in 2006, and serological tests conducted in South Korea using preserved sera from dogs revealed indications of H3N2 CIV as early as 2005 [11, 12]. This chronology aligns with the analysis of H3N2 CIV isolates from Asia that have been sequenced, indicating the presence of a single common ancestor virus in dogs between 1999 and 2006 (95% greatest posterior density) [6]. Since then, South Korea and China have both shown a frequent isolation of H3N2 CIVs in dogs, suggesting that this virus is steadily spreading among canines across Asia [13–17].

H3N2 CIV viruses have recently spread throughout dog populations in North America, South Korea, and China [18].

In April 2015, the H3N2 CIV that was circulating throughout Asia, emerged in Cook County, Illinois. Since then, H3N2 CIV expanded to multiple states, infecting thousands of canines nationwide [5]. The movement of infected dogs is thought to have contributed to the spread of H3N2 CIV within the US. This is likely due to the networks involved in dog rescue and rehoming, which link the host populations in US dog kennels and shelters [5]. By December 2021, cases associated with H3N2 CIV had been documented in the United States, Canada, China, South Korea, and Thailand. The resurgence of CIV in the United States in 2023, particularly in Philadelphia, North Texas, California, and Florida, is therefore unsurprising [19].

Currently, the precise path taken by H3N2 CIV to enter the United States is unknown. On the other hand, the virus most likely stays contagious on fomites for 12 to 48 hours, although an infected dog mayshed the virus for up to three weeks [20]. Thus, close dog-dog contact or direct aerosol exchange is likely the most efficient and frequent way for H3N2 CIV transmission, much like it is for other IAVs. Accordingly, canines who were infected carried the virus to the US. It is plausible that infected dogs were imported into the United States through rescue operations from live animal markets or dog meat farms in South Korea, where H3N2 CIV seroprevalence has been reported at rates ranging from ~ 19% to 100% in individual farms [20].

The aim of the present study was to evaluate the evolution and transmission dynamics of CIV from companion dogs in Alabama, USA. To achieve this, we conducted a comprehensive genomic analysis of H3N2 CIV, with a specific focus on elucidating evolutionary dynamics, temporal patterns, and geographical transmission routes. The whole genome sequences of five H3N2 strains, along with a dataset comprising 100

complete genomes from the Global Initiative on Sharing Avian Influenza Data (GISAID) were used to estimate the evolutionary rates, assess potential reassortment events, and reconstruct the temporal and spatial dissemination patterns leading to the outbreak in Alabama [21, 22]. Our findings provide insights into the epidemiology of H3N2 CIV and may inform future surveillance and control strategies.

RESULTS

Canine influenza virus H3N2 is known to spread rapidly across regions and to evolve through reassortment, leading to recurring outbreaks in the United States [5]. Understanding where new outbreak strains come from and how they change over time requires combining evolutionary and geographic analyses [6]. An outbreak of acute respiratory disease in companion dogs in Alabama was investigated in this study. Nasal swabs from dogs (n = 27) with acute respiratory disease were submitted by veterinarians at the Auburn University College of Veterinary Medicine to the Molecular Diagnostic Laboratory at the Auburn University College of Veterinary Medicine between August and October 2022 for canine influenza virus (CIV) diagnostic testing. Samples of 5 animals were influenza-positive by Real Time RT PCR. These samples were then sequenced by Illumina (iSeq100), and partial or whole genome sequences were generated. Time-scaled phylogenetic, phylodynamic, and phylogeographic approaches were deployed to trace the origins, spread, and reassortment patterns of the outbreak.

Time-Scaled Phylogenetic Reconstruction and Evolutionary Rates

A comparative analysis of evolutionary rates and time to the most recent common ancestor (TMRCA) for individual gene segments of the CIV strains isolated in Alabama was performed using a Bayesian phylodynamic framework. The visualization, employing a whisker plot (Fig. 1), depicts the mean time to the most recent common ancestor and their corresponding 95% highest posterior density intervals (HPDI) for each gene segment (PB2, PB1, PA, NS, NP, NA, MP, and HA) introduced in Alabama. Notably, the polymerase complex genes, PB2, PB1, and NA, exhibited an earlier TMRCA and wider HPDI ranges (95% HPDI = 2019.59–2021.34) compared to the more recently introduced segments in Alabama (95% HPDI = 2021.34–2022.07).

Phylogeographic Origins of The Alabama H3N2 CIV Outbreak

To elucidate the evolutionary context of the five H3N2 CIV isolates from Alabama, a comprehensive phylogenetic analysis was conducted, incorporating a global dataset of

H3N2 CIV strains collected between 2013 and 2022. Maximum clade credibility (MCC) trees were reconstructed for each of the eight individual genomic segments, allowing for a detailed examination of evolutionary relationships across the entire viral genome. The resulting phylogenies consistently demonstrated a tight clustering of the five Alabama H3N2 CIV strains across all gene segments. (Fig. 2, Supplementary Fig. S1).

Within-State Transmission Dynamics in Alabama

The maximum clade credibility tree was inferred from HA and NA genes sequences including CIV (H3N2) sequences from Alabama. The discrete phylogeographic modeling was performed from sequences stamped with date and location information, allowing the reconstruction of the viral transmission dynamics that led to the CIV outbreaks in Alabama. Viral phylogenies exhibit geographical structure compatible with viral transmission from California to Alabama for the HA, MP, NP, NS and PA (location posterior probability (LPP) = 0.83, 0.99, 0.91, 1, 0.99 respectively), from Florida to Alabama for NA (LPP = 0.76), and from Illinois to Alabama for PB1 and PB2 gene segments (LPP = 0.52 and 0.39); Fig. 3 and Supplementary Fig. S2).

Genomic Reassortment Driving Emergence of the Alabama Outbreak Strain

Our analysis revealed a discordant pattern in the genealogy of the viral genes within the Alabama outbreak strains. This incongruence in the evolutionary relationships of distinct viral genes strongly suggests a reassortment event between CIV from California, Florida, and Illinois which led to the emergence of the novel H3N2 strain identified in the Alabama outbreak (Fig. 4).

DISCUSSION

The recent outbreak of H3N2 CIV in Alabama presents a compelling case study for the potential role of reassortment in shaping canine influenza epidemiology. The low immunization rates in the canine population [23] further underscores the vulnerability to novel CIV strains.

The processes underlying virus outbreak epidemiology and cross-species transmission are critical areas of viral evolution. By studying viruses involved in emerging animal outbreaks, we can gain valuable insights into the fundamental mechanisms that facilitate host jumps and the subsequent establishment of viral variants as zoonotic pathogens. Different factors influenced the divergent evolutionary trajectories of CIV, their host-specific adaptations, and global dissemination patterns. A comprehensive understanding

of the evolutionary history and host-specific adaptations of these viruses is essential to assess their potential zoonotic risk to humans.

We performed phylodynamic modeling of the outbreak viral sequences and observed a robust clustering of Alabama CIV strains in each individual gene tree, strongly suggesting a recent common ancestry and localized evolution of these Alabama isolates, distinct from other global H3N2 CIV lineages circulating during the same period. PB2 and NA were estimated to have been circulating in Alabama approximately one year earlier than the remaining segments.

Our phylodynamic inference suggests that reassortment events likely played a key role in the emergence and spread of the H3N2 CIV diversity that led to the outbreak in Alabama. We identified distinct origins for different gene segments of the Alabama outbreak strains. While the HA, MP, NP, NS and PA genes exhibited a phylogenetic relationship with California strains, the PB1, and PB2 genes displayed closer association with strains circulating in Illinois, while NA clustered closely with strains from Florida. This discordant pattern in the genealogy of different viral genes strongly suggests that reassortment events occurred, potentially during co-infection of dogs with viruses from these three geographically distinct sources leading to the generation of the novel H3N2 CIV strain responsible for the Alabama outbreak. The introduction of viruses from California, Florida, and Illinois into Alabama suggests the movement of infected dogs between these regions, or from these regions to Alabama, or an unsampled location. The observed reassortment events in our study could potentially be attributed to canine mobility patterns, particularly within the United States. While precise statistics on dog movement are limited due to a lack of significant economic drivers for tracking, the high degree of human mobility within the U.S. suggests the concomitant movement of companion animals. This is further compounded by the prevalence of pet ownership among college students, who frequently travel between their home states and university towns, potentially facilitating the introduction of pathogens into new geographic areas. Although anecdotal, the movement of show dogs, while representing a small fraction of the overall canine population, may also contribute to long-distance dispersal. Another theory attributable to the movement of infected canines, could be fomite transmission among sheltered dogs from across the country. This spread is hypothesized to occur primarily through interconnected networks involved in canine rescue and rehoming, effectively linking host populations within U.S. kennels and shelters [5]. In contrast, the animals included in our study lacked documented recent travel information, suggesting local infection as the primary source. However, the broader context of canine movement, especially in the U.S., should be considered when interpreting the observed reassortment events [5, 24]. We have observed a similar pattern of introduction and subsequent circulation in equine influenza virus (EIV). For instance, the H3N8 EIV was first isolated in Florida in 1963 and resulted in displacement of the previously circulating H7N7, likely introduced through infected horses from South

America. Descendants of this virus continue to circulate in equine populations nowadays [25]. The historical isolation of swine from widespread influenza transmission, unlike humans and horses, shifted dramatically with the advent of large-scale industrial pig farming in the late 20th century. This transition, coupled with the long-distance transport of pigs within North America, facilitated the rapid dissemination of swine influenza virus (IAV-S) [26]. Moreover, the international trade of live swine, driven by global protein demands, has become a significant driver of IAV-S spread, introducing diverse viral lineages into new regions, particularly in Asia, and leading to increased viral diversity and subsequent challenges in controlling swine flu.

The findings presented here highlight the importance of continued surveillance for CIV, particularly in settings where dogs interact (dog parks) or are housed in close proximity, such as shelters and breeding facilities, which poses vulnerability for dog populations. Shelters and stray dog populations are a particular challenge since densely populated environments and frequent dog-to-dog contact can act as hotspots for viral transmission and potentially facilitate further reassortment events and contribute to the ongoing adaptation and evolution of the virus.

Our study primarily focused on the genetic analysis of the viral strains circulating during the Alabama outbreak. Future investigations could benefit from incorporating additional data sources and information on dog movement patterns, to provide a more comprehensive understanding of the outbreak dynamics. The introduction of influenza strains from geographically distinct locations coupled with the lack of widespread vaccination in the canine population, created conditions conducive to reassortment and generation of new viral diversity.

In conclusion, the findings from the Alabama H3N2 CIV outbreak strongly suggest that reassortment events play a critical role in the emergence and spread of the virus. This case study underscores the importance of continued vaccination and surveillance for influenza virus evolution in canines and the potential public health implications of reassortment events in zoonotic influenza viruses.

METHODS

Sample Collection and RNA Extraction

Nasal swabs from dogs (n = 27) with acute respiratory disease were submitted to the Molecular Diagnostic Laboratory at the Auburn University College of Veterinary Medicine between August and October of 2022 for CIV diagnosis. Total nucleic acids were extracted from nasal swabs using the High-Pure PCR Template Preparation Kit as described [27], followed by fluorescence resonance energy transfer (FRET) PCRs targeting matrix (MP)

gene to detect nucleic acids of CIV [27]. Table 1 includes information about influenza-positive animals. None of the 5 positive animals was vaccinated against CIV.

Table 1
Canine Influenza Virus (CIV) Case Information and Viral Load in Alabama Dogs

Case-1	Submission date and animal location	Breed, sex of the dog	Reason(s) for visit	Influenza virus copies
	August 24, 2022; Deatsville of AL	**Beagle mix, male/castrated**	**Fever, short rapid breathing, not eating/drinking, lethargic**	**26,730/swab**
Case-2	September 8, 2022; Phenix City of AL	Border Collie, male/castrated	Coughing, Snorting	20,160/swab
Case-3	September 12, 2022; Cusseta of AL	Mixed breed, male/castrated	Coughing, vomiting	110,000/swab
Case-4	September 18, 2022; Opelika of AL	Mixed breed, female/spayed	Coughing	165,840/swab
Case-5	September 19, 2022; Auburn of AL	Golden retriever, male/castrated	Labored breathing, unable to walk, respiratory distress	92,040/swab

cDNA Synthesis

Complementary DNA (cDNA) synthesis was performed using SuperScript™ III Reverse Transcriptase (Life Technologies, USA). A total of 100 ng of extracted RNA was combined with the Uni-12 primer (5′-AGCAAAAGCAGG-3′) and subjected to an initial denaturation at 65°C for 5 minutes, followed by immediate cooling on ice for 1 minute. Subsequently, RNaseOUT™ Recombinant Ribonuclease Inhibitor (Life Technologies, USA) and SuperScript™ III Reverse Transcriptase were added to the reaction mixture. Reverse transcription was conducted at 55°C for 60 minutes and terminated by heat inactivation at 70°C for 15 minutes.

CIV Genome Amplification

Amplification of the CIV genomes was conducted using 25 µL of Phusion™ High-Fidelity PCR Master Mix (Thermo Fisher Scientific, USA) in conjunction with IAV gene-specific primers. The primers used included: MBTUni-12 (5′-ACGCGTGATCAGCRAAAGCAGG-3′), MBTUni-13 (5′-ACGCGTGATCAGTAGAAACAAGG3-3′), PB2-1 (5′-

AGCRAAAGCAGGTCAATTATATTCA-3′), PB2-2341R (5′-AGTAGAAACAAGGTCGTTTTTAAACTA-3′), PB1-1 (5′-AGCRAAAGCAGGCAAACCATTTGAATG-3′), PB1-2341R (5′-AGTAGAAACAAGGCATTTTTTCATGAA-3′), PA-1 (5′-AGCRAAAGCAGGTACTGATYCGAAATG-3′), and PA-2233R (5′-AGTAGAAACAAGGTACTTTTTTGGACA-3′), each at a final concentration of 0.1 µM. The reaction mixture also included 5 µL of cDNA and 12 µL of nuclease-free water, bringing the final volume to 50 µL. PCR amplification was conducted under the following thermal cycling conditions: initial denaturation at 98°C for 30 seconds; 10 cycles of 98°C for 10 seconds, 45°C for 30 seconds, and 72°C for 90 seconds; followed by 20 cycles of 98°C for 10 seconds, 58°C for 30 seconds, and 72°C for 30 seconds. A final extension was performed at 72°C for 10 minutes. Post-amplification, DNA products were purified using sparQ PureMag Beads (Quantabio, USA) to remove residual impurities and prepare samples for downstream applications.

Library Preparation and Sequencing

Library preparation for next-generation sequencing was carried out using the Nextera™ DNA Flex Library Preparation Kit (Illumina®, USA), following the manufacturers protocol. Libraries were pooled and loaded onto an iSeq 100 i1 cartridge (Illumina®) for sequencing. Sequencing was performed using multiplexed, paired-end reads across 300 cycles, ensuring high-depth genomic coverage. Consensus sequences for the five individual CIV samples were generated through bioinformatics analysis of FASTQ files. This analysis was performed using the web-based INSaFLU platform, to generate consensus sequences [29].

Study sequence datasets and compilation of background datasets

We used Illumina® next generation sequencing (NGS) technology to generate five canine influenza H3N2 viruses; two complete genomes (complete coding-region of eight gene segments), one near complete (seven complete gene segments and HA partial segment length, 1054 nt), and two partial genomes (two complete coding segments of MP and NS, and partial sequences of HA [1555, 671, 662 nucleotides (nt)], NP [787 nt], PA [950, 820 nt], and PB1 [887, 825 nt] genes). A total of 100 complete CIV genomes were obtained in May 2024 from the GISAID (https://gisaid.org) [30] using the Basic Local Alignment Search Tool [https://blast.ncbi.nlm.nih.gov] for nucleotide sequences available in the EpiFlu interface, based on the lowest e-value.

Multiple sequence alignment, assessment of temporal signal, and phylodynamic reconstruction

We used MUSCLE in Aliview [31] to generate individual alignments for each segment: PB2 (2,277 nucleotides [nt]), PB1 (2,271 nt), PA (2,148 nt), HA (1698 nt), NP (1,494 nt), NA (1,407 nt), NS (837 nt), and MP (756 nt). Alignments were manually edited using Aliview [31]. To infer phylogenetic trees, both maximum-likelihood and Bayesian inference approaches were applied by using web-based IQ-Tree [32] and BEAST v 1.10.4 [33], respectively.

The best-fit nucleotide substitution model was determined by IQ-Tree [34] and applied to all segments. TempEst [http://tree.bio.ed.ac.uk/software/tempest/] was used to detect the temporal signal and identify sequence outliers that were subsequently removed [35].

The overall rates of evolutionary change (substitutions per site per year (subs/site/year)) and the time of the most recent common ancestor (TMRCA) were estimated using BEAST [33], assuming a Bayesian Skygrid coalescent prior [36, 37], with GTR + G+I nucleotide substitution model, and a relaxed uncorrected exponential lognormal clock. The phylogeographic inference was specified using asymmetric Markov model for inference of discrete trait evolution [38].

All chains were run for 100,000,000 generations and logged every 10,000th. At least 10% burn-in was excluded and runs were combined using LogCombiner. Maximum clade credibility trees were summarized using TreeAnnotator and visualized in FigTree [39] and ggtree [40] Transmission dynamics was visualized using ggmap [41].

Declarations

ACKNOWLEDGEMENTS

The opinions expressed in this article are those of the authors and do not reflect the view of the National Institutes of Health, the Department of Health and Human Services, or the United States government.

This work was not explicitly funded by the National the National Institute of Allergy and Infectious Diseases (NIAID) Centers of Excellence for Influenza Research and Response (CEIRR), but the following individuals are part of the CEIRR network under the Emory CEIRR (75N93021C00017) SK (Shakiba Kazemian), PJN, MFC and CSK, and the Center for Research on Influenza Pathogenesis and Transmission (CRIPT) CEIRR (75N93021C00014) NST.

FUNDING DECLARATION

The authors received no specific funding for this work.

AUTHOR CONTRIBUTIONS

CW, MFC, AP, PW, and CSK conceived the experiments, SK (Shakiba Kazemian), PJN, KZ and KC conducted the experiments, SK (Shakiba Kazemian), ST, SK (Samiah Kanwaz), NST and CSK analyzed the results. SK (Shakiba Kazemian), ST, PJN, CW, NST and CSK wrote and edited the manuscript. All authors reviewed the manuscript.

ADDITIONAL INFORMATION

The authors declare no competing interests.

DATA AVAILABILITY

All datasets analyzed during the current study are available from the corresponding author upon reasonable request. Additionally, complete gene segments have been uploaded on GenBank and accession numbers can be found on Supplementary Table 1.

ETHICS DECLARATIONS

The diagnostic samples analyzed in this study were archival specimens originally submitted for routine clinical diagnostic purposes. Their subsequent use in this research project did not require approval from an Institutional Animal Care and Use Committee (IACUC) or equivalent ethics committee, in accordance with established guidelines. This determination is based on the following conditions:

1. No animals were procured, handled, or subjected to procedures specifically for this research.

2. All samples were fully anonymized prior to analysis, with no possibility of linking the data to the original animal clients or specific patient identities.

3. The research constituted a retrospective analysis of existing, de-identified material.

Therefore, under standard ethical and institutional policies that waive IACUC review for such use of anonymous diagnostic archives, this work was exempt.

References

1. Dubois, J., Terrier, O. & Rosa-Calatrava, M. Influenza viruses and mRNA splicing: doing more with less. *mBio* **5**, e00070–e00014 (2014).
2. Breen, M., Nogales, A. & Baker, S. F. Martínez-Sobrido, L. Replication-competent influenza A viruses expressing reporter genes. *J. Virol.* **90**, 179 (2016).
3. Shao, W., Li, X., Goraya, M. U., Wang, S. & Chen, J. L. Evolution of influenza A virus by mutation and re-assortment. *Int. J. Mol. Sci.* **18**, 1650 (2017).

4. Lampejo, T. Influenza and antiviral resistance: an overview. *Eur. J. Clin. Microbiol. Infect. Dis.* **39**, 1201–1208 (2020).
5. Voorhees, I. E. et al. Spread of canine influenza A (H3N2) virus, United States. *Emerg. Infect. Dis.* **23**, 1950–1951 (2017).
6. Zhu, H., Hughes, J. & Murcia, P. R. Origins and evolutionary dynamics of H3N2 canine influenza virus. *J. Virol.* **89**, 5406–5418 (2015).
7. Li, G. et al. Genetic and evolutionary analysis of emerging H3N2 canine influenza virus. *Viruses* **10**, 1–15 (2018).
8. Trovão, N. S., Khan, S. M., Lemey, P., Nelson, M. I. & Cherry, J. L. Comparative evolution of influenza A virus H1 and H3 head and stalk domains across host species. *mBio* **15**, e02649–e02623 (2024).
9. Payungporn, S. et al. Influenza A virus (H3N8) in dogs with respiratory disease, Florida. *Emerg. Infect. Dis.* **14**, 902–904 (2008).
10. Song, D. et al. Transmission of avian influenza virus (H3N2) to dogs. *Emerg. Infect. Dis.* **14**, 741–746 (2008).
11. Li, S. et al. Avian-origin H3N2 canine influenza A viruses in southern China. *Emerg. Infect. Dis.* **16**, 1286–1288 (2010).
12. Lee, Y. et al. Serologic evidence of H3N2 canine influenza virus infection before 2007. *Vet. Rec*. **171**, 44 (2012).
13. Lin, Y., Zhao, Y., Zeng, X., Lu, C. & Liu, Y. Genetic and pathobiologic characterization of H3N2 canine influenza viruses isolated in the Jiangsu province of China in 2009–2010. *Vet. Microbiol.* **158**, 247–258 (2012).
14. Wang, H. et al. Genetic characterization of avian-origin H3N2 canine influenza viruses isolated from Guangdong during 2006–2012. *Virus Genes*. **46**, 558–562 (2013).
15. Teng, Q. et al. Characterization of an H3N2 canine influenza virus isolated from Tibetan mastiffs in China. *Vet. Microbiol.* **162**, 345–352 (2013).
16. Su, S. et al. Avian-origin H3N2 canine influenza virus circulating in farmed dogs in Guangdong, China. *Emerg. Infect. Dis.* **19**, 444–449 (2013).
17. Yang, X. et al. Identification and genetic characterization of avian-origin H3N2 canine influenza viruses isolated from Liaoning province of China in 2012. *Virus Genes*. **49**, 342–347 (2014).
18. Borland, S., Gracieux, P., Jones, M., Mallet, F. & Yugueros-Marcos, J. Influenza A virus infection in cats and dogs: a literature review in the light of the one health concept. *Front. Public. Health*. **8**, 83 (2020).
19. Oduoye, M. O. et al. Molecular epidemiology of canine influenza virus in Nigeria. *J. Glob Infect. Dis.* **6**, e0191 (2023).

20. Lee, C. et al. A serological survey of avian-origin canine H3N2 influenza virus in dogs in Korea. *Vet. Rec*. **137**, 359–362 (2009).
21. Elbe, S. & Buckland-Merrett, G. Data, disease and diplomacy: GISAID's innovative contribution to global health. *Glob Chall.* **1**, 33–46 (2017).
22. Shu, Y. & McCauley, J. G. I. S. A. I. D. Global initiative on sharing all influenza data – from vision to reality. *Euro. Surveill*. **22**, 30494 (2017).
23. Day, M. J., Horzinek, M., Schultz, R. & Squires, R. WSAVA guidelines for the vaccination of dogs and cats. *J. Small Anim. Pract.* **57**, E1–E45 (2016).
24. Newbury, S. et al. Prolonged intermittent virus shedding during an outbreak of canine influenza A H3N2 virus infection in dogs in three Chicago area shelters: 16 cases (March to May 2015). *J. Am. Vet. Med. Assoc.* **248**, 1022–1026 (2016).
25. Chambers, T. M. Equine influenza. *Cold Spring Harb Perspect. Med.* **12**, a038331 (2022).
26. Trovão, N. S. & Nelson, M. I. When pigs fly: pandemic influenza enters the 21st century. *PLoS Pathog*. **16**, e1008259 (2020).
27. Luan, L. et al. Detection of influenza A virus from live-bird market poultry swab samples in China by a pan-IAV, one-step reverse-transcription FRET-PCR. *Sci. Rep.* **6**, 30015 (2016).
28. Hoffmann, E., Stech, J., Guan, Y., Webster, R. & Perez, D. Universal primer set for the full-length amplification of all influenza A viruses. *Arch. Virol.* **146**, 2275–2289 (2001).
29. Borges, V., Pinheiro, M., Pechirra, P., Guiomar, R. & Gomes, J. P. INSaFLU: an automated open web-based bioinformatics suite from-reads for influenza whole-genome-sequencing-based surveillance. *Genome Med.* **10**, 46 (2018).
30. Khare, S. et al. GISAID's role in pandemic response. *Lancet* **3**, 1049–1051 (2021).
31. Larsson, A. AliView: a fast and lightweight alignment viewer and editor for large datasets. *Bioinformatics* **30**, 3276–3278 (2014).
32. Trifinopoulos, J., Nguyen, L. T., von Haeseler, A. & Minh, B. Q. W-IQ-TREE: a fast online phylogenetic tool for maximum likelihood analysis. *Nucleic Acids Res.* **44**, W232–W235 (2016).
33. Suchard, M. A. et al. Bayesian phylogenetic and phylodynamic data integration using BEAST 1.10. *Virus Evol.* **4**, vey016 (2018).
34. Minh, B. Q. et al. IQ-TREE 2: new models and efficient methods for phylogenetic inference in the genomic era. *Mol. Biol. Evol.* **37**, 1530–1534 (2020).
35. Rambaut, A., Lam, T. T., Carvalho, M., Pybus, O. G. & L. & Exploring the temporal structure of heterochronous sequences using TempEst (formerly Path-O-Gen). *Virus Evol.* **2**, vew007 (2016).

36. Hill, V. & Baele, G. Bayesian estimation of past population dynamics in BEAST 1.10 using the Skygrid coalescent model. *Mol. Biol. Evol.* **36**, 2620–2628 (2019).
37. Kaplan, B. S. et al. Aerosol transmission from infected swine to ferrets of an H3N2 virus collected from an agricultural fair and associated with human variant infections. *J. Virol.* **94**, e01009–e01020 (2020).
38. Edwards, C. J. et al. Ancient hybridization and an Irish origin for the modern polar bear matriline. *Curr. Biol.* **21**, 1251–1258 (2011).
39. Rambaut, A. FigTree v1.3.1. (2010). http://tree.bio.ed.ac.uk/software/figtree
40. Yu, G. et al. ggtree: an R package for visualization and annotation of phylogenetic trees with their covariates and other associated data. *Methods Ecol. Evol.* **8**, 28–36 (2017).
41. Kahle, D. & Wickham, H. ggmap: spatial visualization with ggplot2. *R J.* **5**, 144–161 (2013).

Figures

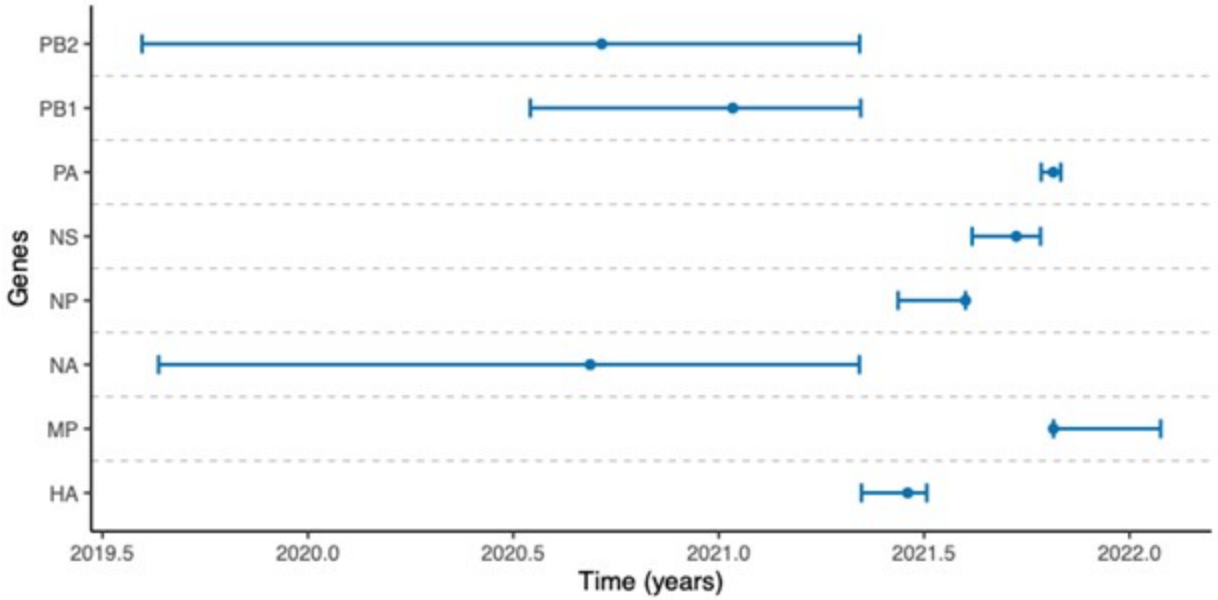

Figure 1

Estimates of the time to the most recent common ancestor and mean nucleotide substitution rates for the eight gene segment of CIV H3N2 introduced in Alabama. Bayesian time-scaled phylogenetic analyses were performed on all eight genomic segments using BEAST to estimate the time to the most recent common ancestor (tMRCA) and mean nucleotide substitution rates for Alabama H3N2 CIV isolates. Posterior mean estimates are shown with 95% highest posterior density intervals. The analyses reveal

recent common ancestry among Alabama strains and segment-specific evolutionary rate variation, consistent with rapid local diversification following viral introduction.

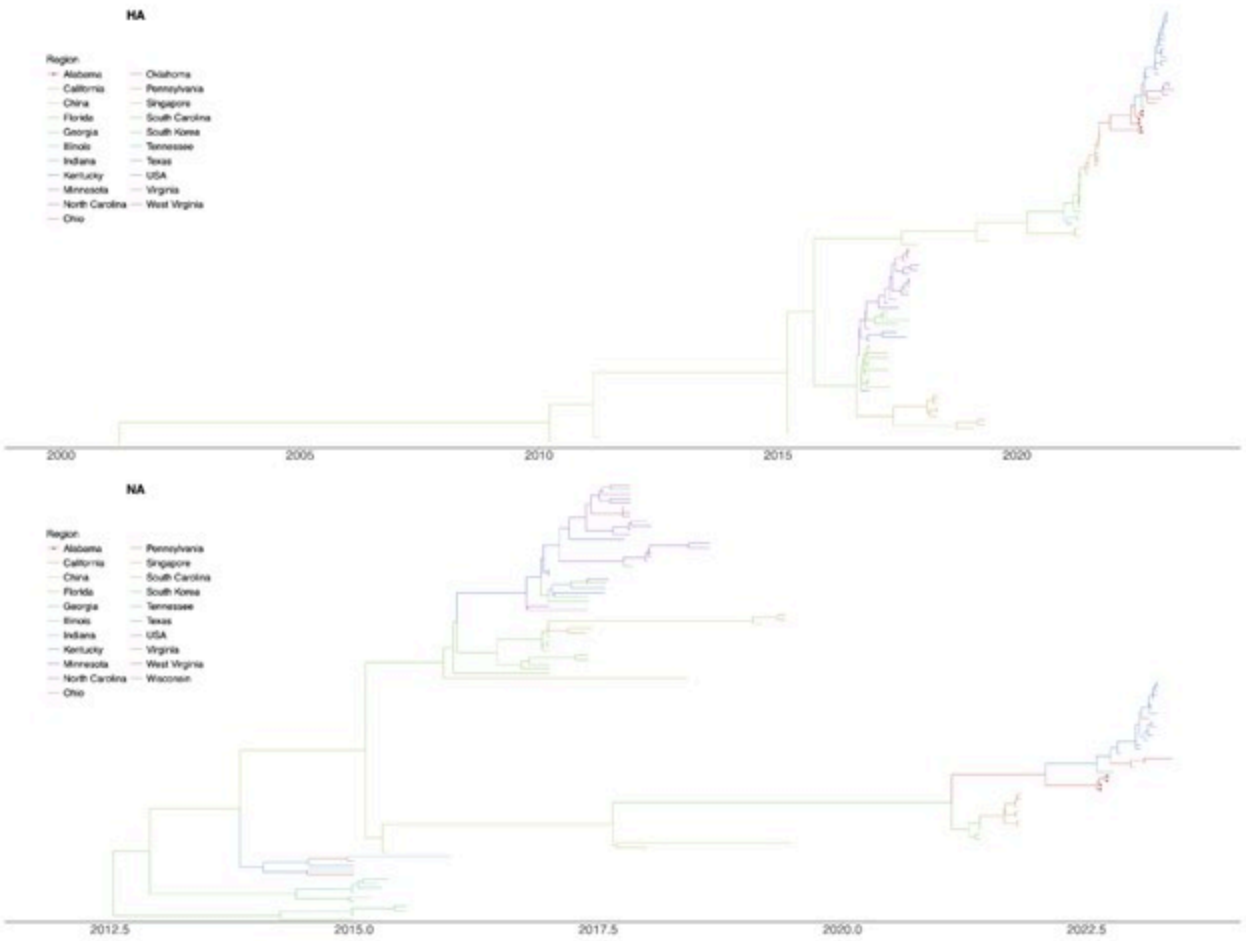

Figure 2

Discrete phylogeographic maximum clade credibility trees of CIV (H3N2) based on the nucleotide sequence of the HA and NA genes. Discrete phylogeographic maximum clade credibility trees were inferred for the HA and NA genes to reconstruct the geographic ancestry of the Alabama outbreak strain. Branch colors indicate inferred source states, and node support values represent posterior probabilities. The trees demonstrate distinct ancestral origins of HA and NA segments, suggesting multiple interstate introductions contributing to the Alabama outbreak. The location of the most likely ancestor of the descendant tips determines the color of the ancestral nodes and branches, which are time-scaled in years.

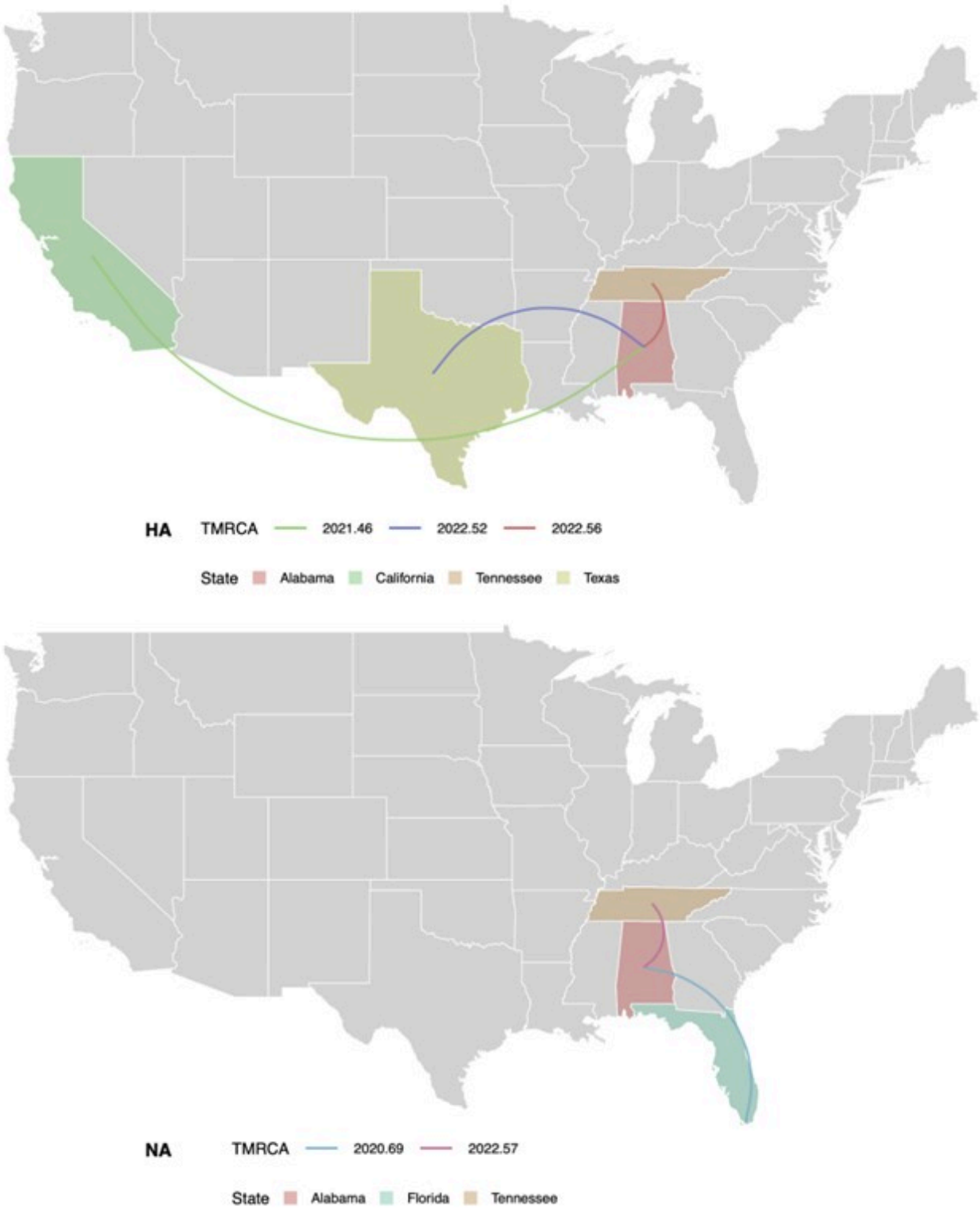

Figure 3

Bayesian Phylogeographic Reconstruction of CIV Spread in Alabama. Spatiotemporal dissemination of CIV H3N2 among domestic dogs determined by Bayesian discrete phylogeographic inference of HA and NA genes segments. Curves show the interstate virus lineage transitions with time to the most recent common ancestor. The panel above shows the transition of HA gene from California to Alabama, and subsequent transmission

from Alabama to Texas and Tennessee. The lower panel shows the transition of NA gene from Florida to Alabama and subsequent transmission from Alabama to Tennessee. The curves connecting different states indicate the direction (concave - westwards and convex - eastwards) and estimated timing of viral lineage movement between those locations.

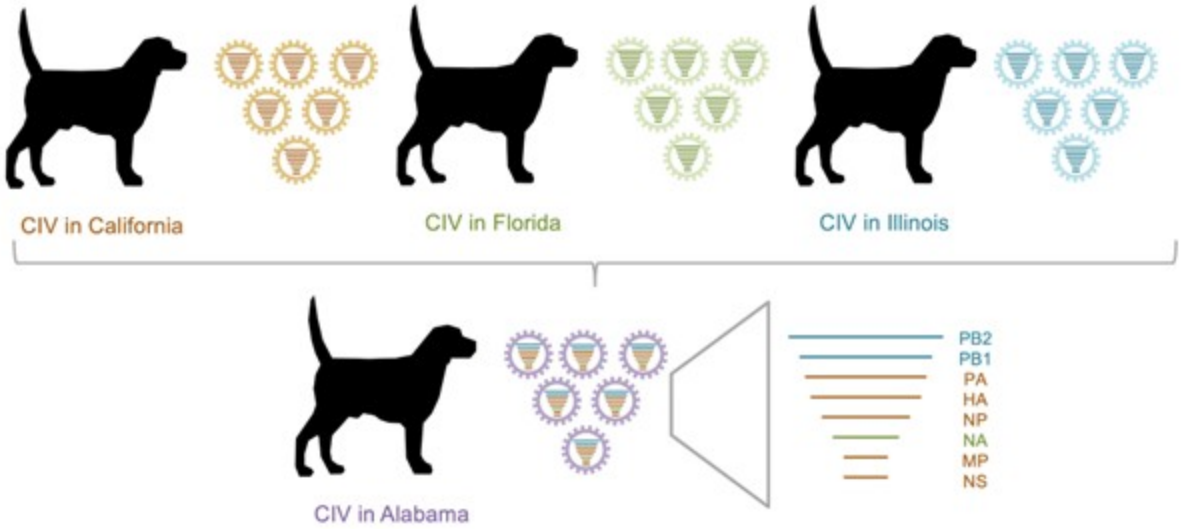

Figure 4

Reassortment of Canine Influenza Virus in Alabama. Phylogeographic reconstructions suggest a reassortment event that led to the emergence of a novel H3N2 CIV strain in Alabama. The ancestral lineages for the Hemagglutinin (HA), Matrix Protein (MP), Nucleoprotein (NP), Non-structural protein (NS), and Polymerase Acid (PA) genes of the Alabama outbreak strains originated in California, NA originated in Florida, whereas the Polymerase Basic 1 (PB1) and Polymerase Basic 2 (PB2) genes share a most recent common ancestor with strains circulating in Illinois.

Supplementary Files

This is a list of supplementary files associated with this preprint. Click to download.

- SupplTable1.pdf
- SupplementaryFigureS1.jpeg
- SupplementaryFigureS2.jpeg